Article
Vol. 27, No. 4, p. 385–397, August 2023
https://doi.org/10.1007/s12303-023-0011-z
pISSN 1226-4806 eISSN 1598-7477
Geosciences Journal GJ

Mineralogy, geochemistry, and sources of clay minerals in sediments of the Ulleung Basin, East Sea (Sea of Japan)

Suhyun Kim[1], Hyeonho An[1,3], Changhwan Kim[4], and Kiho Yang[1,2]*

[1]Department of Oceanography, Pusan National University, Busan 46241, Republic of Korea
[2]Department of Oceanography and Marine Research Institute, Pusan National University, Busan 46241, Republic of Korea
[3]Ocean Georesources Research Department, Korea Institute of Ocean Science and Technology (KIOST), Busan 49111, Republic of Korea
[4]East Sea Research Center, Korea Institute of Ocean Science and Technology (KIOST), Uljin 36315, Republic of Korea

ABSTRACT: The provenance of sediments in the Ulleung Basin, East Sea (Sea of Japan), could be attributed to diverse sources, including the Tsushima Warm Current (TWC) and Korean coast. However, the contributions of these sources and their impacts on the composition of clay minerals, the distribution and composition of which can be used to decipher the paleoenvironment and provenance of sediments, remain obscure. Therefore, herein, we aimed to characterize the paleoenvironments and provenance of the sediments from the Ulleung Basin by analyzing their clay mineral compositions using X-ray diffraction and transmission electron microscopy-energy dispersive X-ray spectroscopy. For analysis, sediment cores were obtained during an expedition from March 30 to April 10, 2021, aboard the Onnuri R/V, and these were assigned three provenances: Korean coast, TWC, and a mixture of both. Results showed that clay minerals are abundant in the surface sediments and are dominated by illite (mean = 49.1%). Clay mineral composition changes in a southwest to northeast direction. Sediments sourced from the TWC are poor in smectite and rich in illite. In contrast those assigned a mixed provenance are rich in illite and poor in kaolinite and chlorite. This change is particularly evident toward the Dokdo area (from SW to NE). Moreover, piston core samples from St. 8 and 10 also indicate the presence of plagioclase, microcline, and quartz. We found a rhodochrosite layer in St. 8 samples, at a depth of 3.96 and 4.00 m, which represents the transition from the Last Glacial Maximum (LGM) to the Holocene. Our results indicated that the input of smectite in the basin increased from the LGM to the present whereas that of other clay minerals decreased. The smectite originated mainly from the Korean coast and illite from the TWC. Kaolinite and chlorite in the sediments exhibited similar horizontal and vertical patterns, which are attributed to the interaction between climate, ocean currents, and sediment sources. Moreover, Al- and Fe-rich smectites were observed, compositional variations of which could be attributed to source differences. These results are indicative of other sources of smectites in addition to the three provenances highlighted. This study provides a detailed analysis of sediment sources and horizontal and vertical clay mineral composition changes and shows the difference between them. Sediment from the Ulleung Basin was affected by not only aeolian dust but other factors, such as various sediment sources, ocean circulation, and climate change.

Key words: clay minerals, paleoenvironment, sediment provenance, transmission electron microscopy-energy dispersive X-ray spectroscopy, Ulleung Basin

Manuscript received February 2, 2023; Manuscript accepted March 12, 2023

Editorial responsibility: Tae Soo Chang

***Corresponding author:**
Kiho Yang
Department of Oceanography, Pusan National University, 2, Busandaehak-ro 63beon-gil, Geunjeong-gu, Busan 46241, Republic of Korea
Tel: +82-51-510-2273, E-mail: kyang@pusan.ac.kr

Electronic supplementary material
The online version of this article (https://doi.org/10.1007/s12303-023-0011-z) contains supplementary material, which is available to authorized users.

1. INTRODUCTION

The East Sea (Sea of Japan) is a semi-enclosed marginal sea, and owing to numerous environmental changes during the glacial-interglacial period, sediments in the area are associated with diverse depositional environments. Clay minerals in sediments have attracted attention as indicators of the provenance and depositional environment of sediments due to compositional difference.

The distribution of clay minerals and their significance to provenance in sediments of the East Sea have been reported in many studies (Bahk et al., 2001, 2004; Lee, 2007; Son et al., 2009;

Liu et al., 2010; Lim et al., 2011; Um et al., 2013; Koo et al., 2014; Xu et al., 2014; Lee et al., 2015; Shen et al., 2017). Bahk et al. (2004), for example, reported that the terrigenous components in sediments of cores, obtained from the southern margin of the Ulleung Basin, were affected by hemipelagic riverine sediment fluxes following the Last Glacial Maximum (LGM). Moreover, Xu et al. (2014) indicated that sediment provenance was mainly controlled by sea level changes in the last 21 kyrs. Previous studies suggest that aeolian dust was the main source of sediments to the East Sea (Irino and Tada, 2003; Yokoyama et al., 2006; Nagashima et al., 2011; Sagawa et al., 2018). According to these studies, the input of sediments to the East Sea has alternated from dominantly terrigenous to hemipelagic following the LGM, and these changes were significantly influenced by eolian dust. However, these studies focused on horizontal and vertical variations induced by eolian dust, and thus, the contributions of other factors, such as the Tsushima Warm Current (TWC) and turbidities on the composition of sediments in the basin have remained neglected (Xu et al., 2014; Lee et al., 2021). Shen et al. (2017) also suggested that the clay mineral fractions of sediments in the basin exhibited no discernible trend, and the relative proportions depended on loess and other sources (Fig. S1 in the electronic supplementary material).

Considering the expected horizontal and vertical trends in clay minerals and the effects of detrital particles on the composition of sediments in the Ulleung Basin, in the present study, we characterized these sediments using transmission electron microscopy-energy dispersive X-ray spectroscopy (TEM-EDS). As a type of clay mineral, smectite exhibits compositional differences based on its source, and thus, it is suitable for the characterization of the provenances of sediments. Therefore, TEM-EDS is a technique that can be used to decipher the source of sediments in a basin at a high resolution. The present study improves our understanding of sedimentation in the Ulleung Basin from the LGM period to the Holocene and highlights the potential of smectite for source analysis based on TEM-EDS.

2. GEOLOGICAL SETTING

The present study was conducted in the southwest portion of the Ulleung Basin, which represents one of the three deep basins in the East Sea (Fig. 1; Bahk et al., 2005). The study area is characterized by water depths exceeding 2000 m (Kim and Kim, 2001; Cha et al., 2007; Son et al., 2009), and the associated variation of currents severely impacts the supply of sediments. Among these currents, the TWC, which is a component of the warm saline Kuroshio Current, is the main current that controls flow in the East Sea through the Korean strait (Bahk et al., 2005). Hence, the TWC has impacted the composition of clay minerals in sediments of the basin since the LGM (Xu et al., 2014). The East Korea Warm Current, one of two segments of the TWC, flows along the Korean coast and across the southern part of the

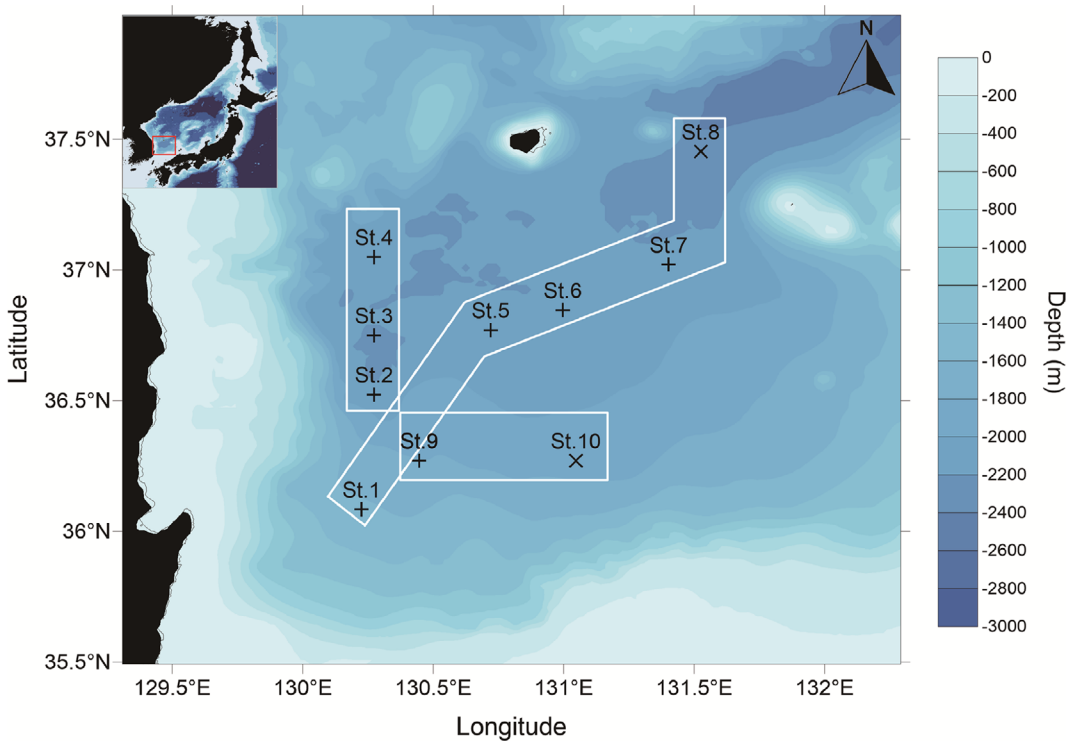

Fig. 1. Illustration showing sites in the Ulleung Basin, East Sea (Sea of Japan) from which samples were collected. The cross (+) represent a multiple-core (MC) site (St. 1, 2, 3, 4, 5, 6, 7 and 9), whereas the (×) denotes a piston-core (PC) site (St. 8 and St. 10).

Ulleung Basin (Mooers et al., 2005; Cha et al., 2007; Park et al., 2013).

In addition to the TWC, terrigenous sources also contribute sediments to the Ulleung Basin. Even though majority of the terrestrial sediments were deposited in the Hupo Basin (Lee et al., 2015), turbidity currents transported some of the sediments to the Ulleung Basin (Kim and Kim, 2001; Bahk et al., 2004; Lee et al., 2021). Mixing of coastal and TWC sediments could also affect the distribution of sediments in the study area, particularly in the center of the basin. Consequently, sediments in the study area are attributed to, at least, three different sources from the Korean coast (turbidities), the TWC, and a mixture of both.

3. MATERIALS AND METHODS

3.1. Sampling of Sediments

Multiple core (MC) and piston core (PC) sediments were collected during an expedition aboard the Onnuri research vessel (RV), from March 30 to April 10, 2021 (Fig. 1). Cores were retrieved from sites associated with three provenances, including the Korean coast, TWC, and a mixture of both. Sites St. 2–St. 4 that were assigned to the Korean coast are along the coast from south to north, whereas sites St. 9 and St. 10 are located from east to west relative to the direction of the TWC. St. 1 and St. 5–St. 8, which represent sediments with a mixed source, are aligned from the southwest to northeast (Fig. 1).

3.2. Mineralogy and Geochemistry Analyses

3.2.1. X-ray diffraction

Samples were collected at intervals of ~30 cm, as well as based on distinct facies from the sediment cores (St. 8 and St. 10), and the < 2 μm fractions were separated for measuring clay mineral assemblages. The clay fraction sample was placed on a glass slide applying the filter-peel method using a 0.45-μm membrane filter paper (Moore and Reynolds, 1989; Kim et al., 2019). The ethylene glycol solvate samples were then placed in a desiccator for 8 h. Subsequently, oriented clay mounts (air-dried) were measured based on 2θ angles that varied from 2° to 30°. The analyses were conducted at a speed of 1.5°/min and a step size of 0.02° using an X'Pert Pro instrument (Korea Institute of Ocean Science and Technology (KIOST), Busan, Korea) that is equipped with a CuKα radiation source (45 kV and 30 mA). Clay minerals were identified using the Crystallographical Search-Match software (version 2.0.3.1), and a semi-quantification method (Biscaye, 1965) was utilized to determine the relative proportions of clay minerals, including smectite, illite, chlorite, and kaolinite.

3.2.2. TEM-EDS

The structural and elemental constituents of the smectite were characterized using lattice fringe imagery, selected-area electron diffraction (SAED), and EDS. The preparation of samples for TEM analyses involved two major steps (Kim et al., 1995). First, the TEM samples were infused with the L.R. White resin to preserve the structure of layers in smectite and other clay minerals because the dehydration of smectite could result in the collapse of its structure when exposed to the high TEM vacuum. The preserved samples were then cut using ultramicrotomy to a thickness of 70 nm (Leica, RM2265, Eulji University, Seongnam, Korea), and each sample was placed on a lacey carbon TEM Cu-grid. TEM analysis was performed using a TALOS F200X at 200 kV (Pusan National University, Busan, Korea), and lattice fringe images and SAED patterns were used to separate the smectite using EDS.

4. RESULTS AND DISCUSSION

4.1. Sedimentary Facies

The MC sediments that were obtained from intervals of approximately 54 cm can be partitioned into an upper red-brown layer and a lower olive-brown homogenous layer (Fig. 2a). The red-brown color of the top part of the upper layer is attributed to deposition in oxic environments. The PC samples that were obtained from St. 8 and St. 10 comprised mud and layers of other sediments, including alternating dark- and light-colored layers and an orange-brown layer (Fig. 2b, c). In contrast to the core from St. 10, the uppermost part of the core from St. 8 involved a brown layer that was linked to oxidation. The most characteristic feature of this core section was the presence of a rhodochrosite layer that is overlain by a dark brown layer, and this occurs at depths between 3.96 and 4.00 m (Bahk et al., 2001). Beneath a depth of 4.00 m, sand and gravel layers were present. The rhodochrosite layer is interpreted to represent the transition from the glacial to the Holocene period (Bahk et al., 2001; Lee et al., 2020), and the sands and gravels indicate terrigenous inputs during the LGM. Therefore, the upper 4.00 m of sediments was deposited after the LGM, and this suggests that the source of sediments changed dominantly from terrigenous to hemipelagic. St. 10 is almost entirely a mud layer, but the very fine sand layer between 2.10 m and 2.20 m depth implies a change in the sediment source.

4.2. Mineralogy of the Sediments

The lateral and vertical distributions of clay minerals were examined to evaluate their significance to the provenance and

https://doi.org/10.1007/s12303-023-0011-z

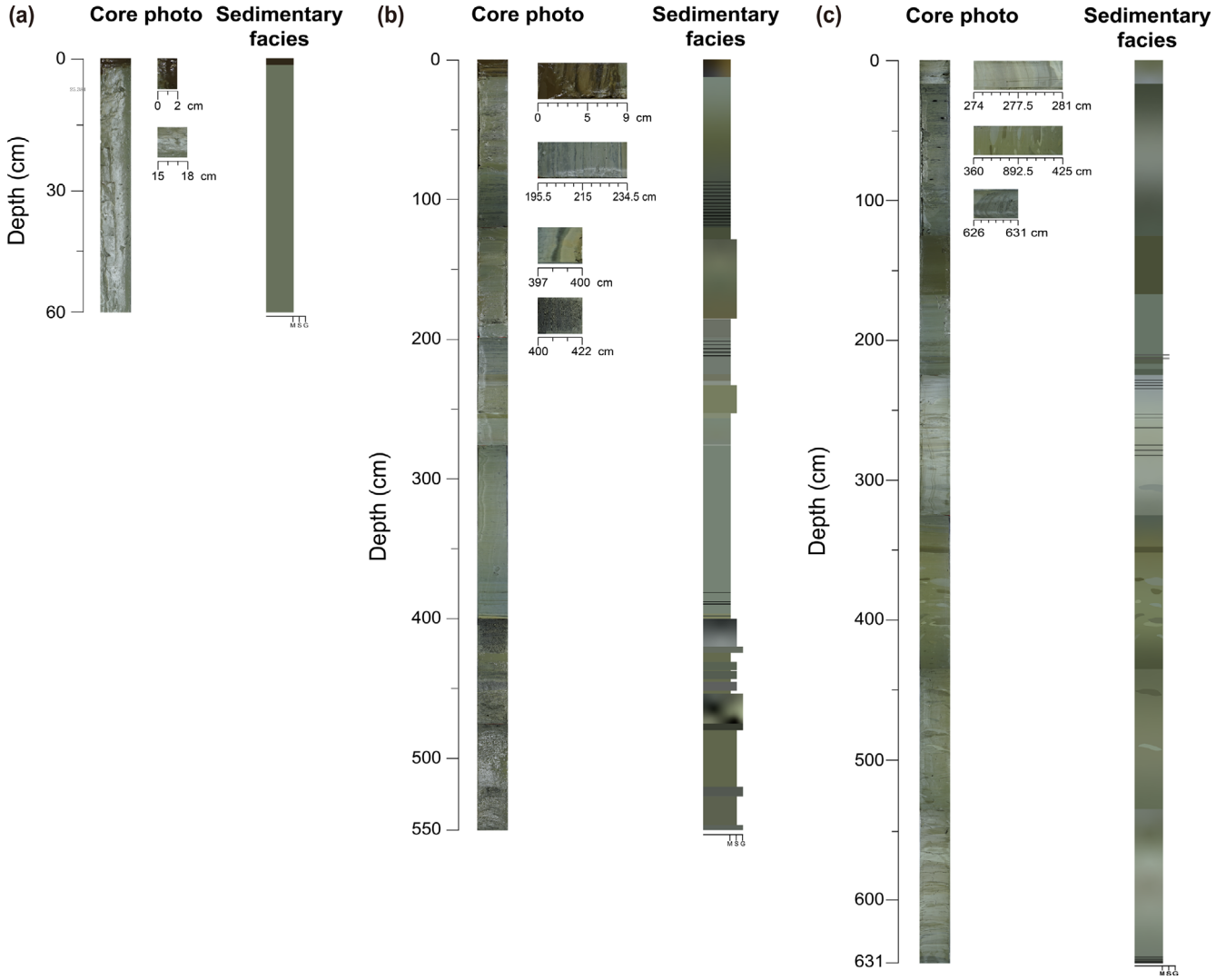

Fig. 2. Profiles showing sedimentary facies in sediments from (a) St. 5, (b) St. 8, and (c) St. 10.

environments of deposition of the sediments. The relative abundance of clay minerals was calculated based on peaks from the XRD analyses of the glycol-treated samples and the method proposed by Biscaye (1965). TEM-EDS was used to characterize the elemental composition of smectite according to sources of the sediments.

4.2.1. Lateral trends of clay minerals

Clay minerals in the sediments include smectite, illite, kaolinite, and chlorite (Fig. 3) and their relative abundances are presented in Table 1. Among these minerals, illite is the most abundant, and its relative proportions vary from 35.9 to 63.4% (mean = 49.1%). In terms of abundance, it is followed by smectite (mean = 34.9%), chlorite (mean = 8.3%), and kaolinite (mean = 7.7%). The sediments from the Korean coast contain predominantly smectite (mean = 37%) whereas those attributed a mixed provenance are dominated by kaolinite and chlorite (mean = 8.9 and 9.3%, respectively), and illite is the most abundant clay mineral in sediments associated with the TWC (mean = 48.2%).

The distribution trends of clay minerals in the sediments vary according to the source (Fig. 4). In sediments from the Korean coast, the proportion of smectite decreased whereas that of other clay minerals increased at St. 2 to St. 5. Regarding samples assigned to a mixed provenance, smectite displayed increasing and decreasing patterns, with other minerals showing opposite trends. The proportion of illite increased for samples from St. 9 to St. 10 whereas that of other clay minerals decreased. In general, the trend of smectite was opposite to those of other clay minerals for samples of the same source, excluding samples assigned to the TWC. These results indicate that the mechanism associated with the input of sediments to St. 9 and St. 10 mainly affected the proportion of illite distribution, and this explains

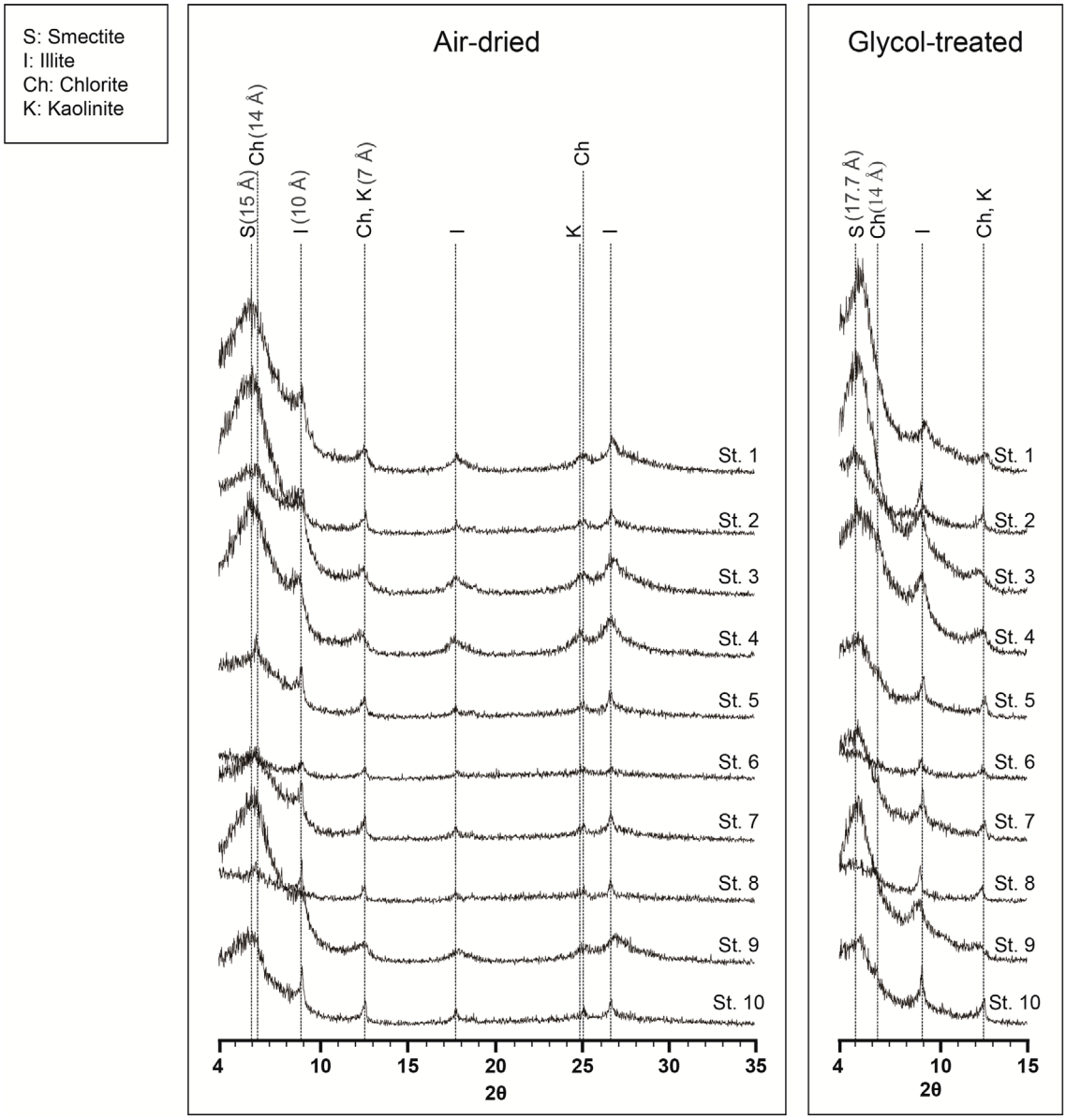

Fig. 3. Representative X-ray diffraction patterns of air-dried and glycol-treated clay minerals in the surface sediments from sampling sites in the present study.

Table 1. Relative abundance of clay minerals in surface sediments from the Ulleung Basin, East Sea (Sea of Japan)

Sample site	Smectite (%)		Illite (%)		Kaolinite (%)		Chlorite (%)	
	avg	std	avg	std	avg	std	avg	std
St. 1	50.0	0.03	35.9	0.14	6.1	0.04	7.9	0.05
St. 2	29.6	0.21	53.0	0.11	7.6	0.05	9.9	0.06
St. 3	44.9	0.05	43.8	0.04	5.8	0.03	5.5	0.03
St. 4	36.5	0.25	47.5	0.2	7.02	0.03	9.0	0.04
St. 5	33.1	0.12	42.0	0.47	13.7	0.33	11.1	0.26
St. 6	20.5	0.22	51.6	0.56	13.8	0.27	14.1	0.28
St. 7	37.1	0.19	48.0	0.18	6.8	0.03	8.1	0.04
St. 8	27.3	0.25	63.4	0.32	4.2	0.06	5.2	0.04
St. 9	42.4	0.07	43.6	0.14	7.2	0.06	6.9	0.05
St. 10	27.4	0.03	62.4	0.06	4.4	0.02	5.8	0.03

Note: avg, average; std, standard deviation.

https://doi.org/10.1007/s12303-023-0011-z

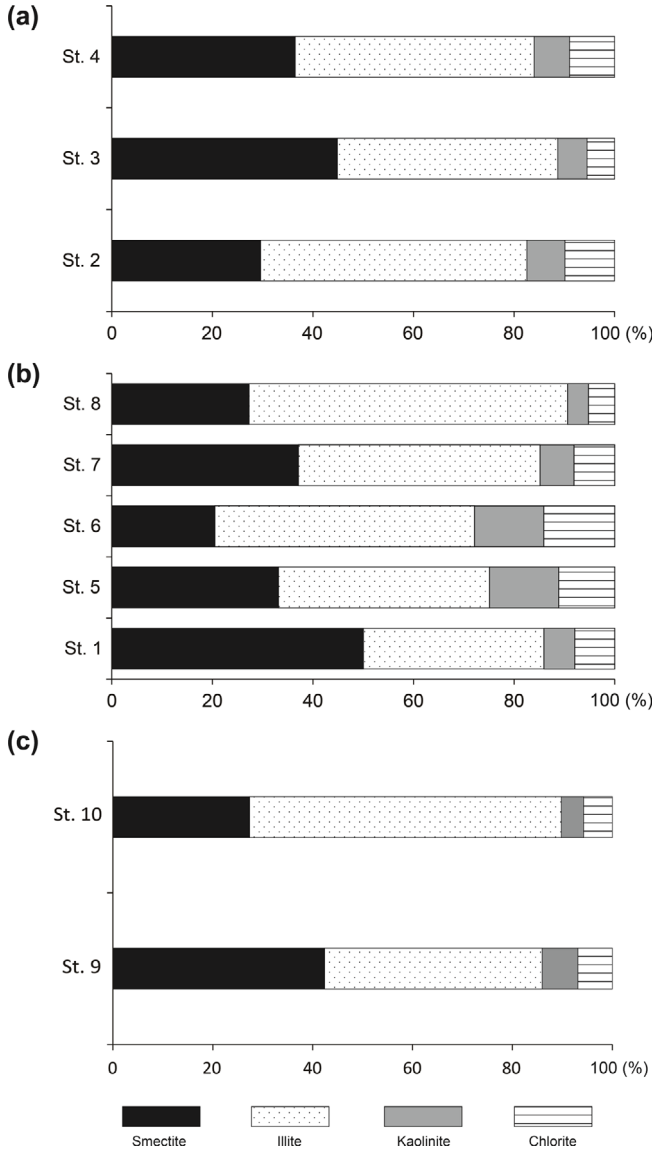

Fig. 4. Plot showing a comparison of the relative abundances of clay minerals in surface sediments from the Ulleung Basin, East Sea (Sea of Japan). The sources of these sediments include the (a) Korean coast, (b) mixture of the Korean coast and Tsushima warm current (TWC), and (c) TWC.

changes in the proportions of other clay minerals.

Owing to the dominance of smectite in samples from sites in the Korean coast, this area was considered as a primary source of smectite in sediments of the study area. Regarding samples of a mixed origin, the proportion of smectite decreased in samples from St. 1 to St. 6 but increased in the sample from St. 7. These results show that authigenic smectite that originated from volcanic rocks in in the Ulleung-do and Dokdo areas was transported and deposited in the study area (Khim et al., 1997; Lee and Kim, 2007). Illite, which is the most abundant clay mineral in samples associated with the TWC, showed an increase in proportion toward the east (from St. 9 to St. 10). Thus, the area under the influence of the TWC was likely a major source of illite to the study area, and this observation is consistent with results from a previous study (Lee, 2007). Rivers in China (Yellow River and Yangtze River) and Taiwan that transport illite-rich sediments probably supplied illite via the Korean Strait, and this impacted the overall distribution of illite in the study area (Shen et al., 2017). The distribution of illite in the study area differs from the expected gradual decrease along the flow path of the TWC, and this explains the low proportion of smectite in samples from St. 10 and direct TWC impact on St. 10 (Park et al., 2013). Kaolinite exhibits a higher relative abundance offshore and in deep portions of the basin than in the coastal and slope areas. This mineral was primarily derived from the Korean strait and its environment (Lee, 2007).

4.2.2. Vertical trends of clay minerals

Vertical profiles of St. 8 and St. 10 reveal the presence of clay minerals, microcline, quartz, and plagioclase (Fig. 5), and the calculated relative abundances of clay minerals are presented in Tables 2 and 3. The clay minerals are dominated by illite (mean = 53.3% for St. 8 and 55.5% for St. 10), followed by smectite (mean = 29.8% for St. 8 and 29.7% for St. 10), kaolinite (mean = 8.5% for St. 8 and 7.1% for St. 10), and chlorite (mean = 8.4% for St. 8 and 7.7% for St. 10).

Figure 6 shows trends in the vertical distribution of clay minerals at St. 8 and St. 10. Both stations are characterized by increasing smectite and decreasing illite, kaolinite, and chlorite proportions toward the present. St. 8 and St. 10 have similar vertical patterns but a higher variability is evident for St. 8.

The transition from the glacial to interglacial period is marked by the presence of rhodochrosite layer at a depth of approximately 4.00 m at St. 8. This layer highlights the change in climate and deglaciation and evolution from the LGM to the Holocene. These changes are reflected by the smectite/(illite + chlorite) ratios of the sediments. Smectite is formed in a warm climate, whereas the other clay minerals are linked to a cool climate, and thus, the high ratios for samples from St. 8 indicate that the area was characterized by a warm climate. The vertical distribution of clay minerals and ratios for St. 10 are similar to those for St. 8, and these even display lower variations.

Owing to the low sea level (−120 m) at the start of the LGM, coarse-grained terrigenous and riverine sediments were deposited to produce sedimentary facies that were observed beneath the rhodochrosite layer at St. 8, whereas such coarse-grained sediments were missing at St. 10. So, following the end of the LGM, deposited sediment shifted from coarse- to fine-grained hemipelagic. The occasional prominent peaks in Figure 6a are attributed to the sudden introduction of sediments with variable compositions.

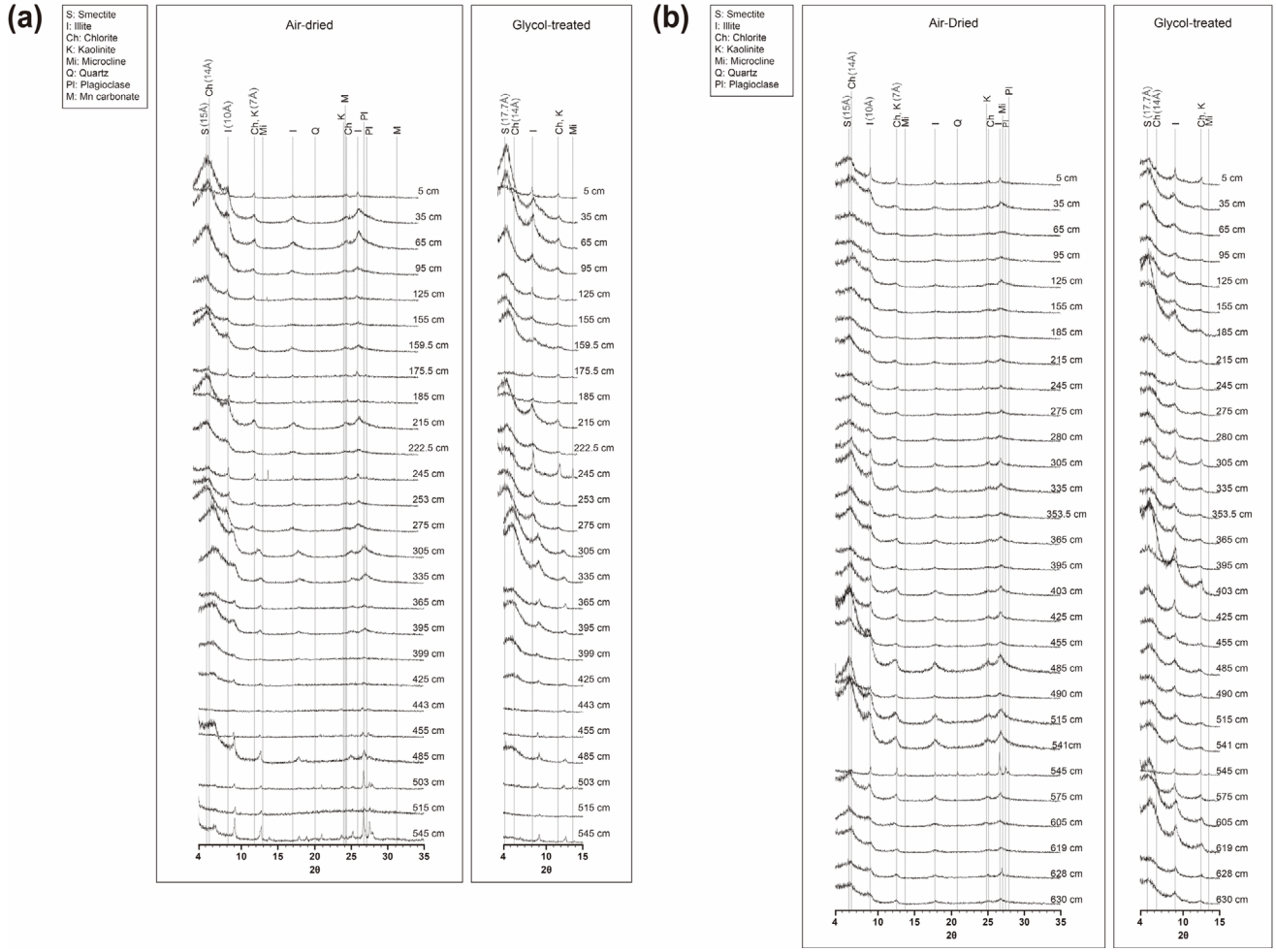

Fig. 5. Representative X-ray diffraction patterns of air-dried and glycol-treated clay minerals in piston-core sediments from (a) St. 8 and (b) St. 10.

Depth at which prominent peaks occur are characterized by low intensities of clay minerals (Fig. 5a) and an afflux of coarse-grained sediments. These sediments probably originated from the Nakdong River, which commonly transports coarse-grained sediments that are richer in kaolinite and chlorite than those from the East Sea (Kwak et al., 2016). According to Bahk et al. (2004), the flux of riverine sand and silt into hemipelagic environments probably affected deposition in the Ulleung Basin during the last deglaciation, and sediments were likely delivered directly from the Korea Strait. It is caused by paleochannels in the Nakdong River extended into the shelf margin during the last sea-level lowstand. Even though data for St. 10 show no prominent peak, sand layers were probably supplied by the Nakdong and Changjiang rivers (Cha et al., 2007).

Even though kaolinite and chlorite in samples from the study area were formed by different mechanisms in diverse environments, the lateral and vertical distributions of both minerals exhibit similarities (Figs. 4 and 6). According to the smectite/(illite + chlorite) ratios (Fig. 6), the area was characterized by a warm climate, and this produced high kaolinite and low chlorite. However, the abundance of both mineral subsequently decreased to the present levels, and these decreases are attributed to changes in ocean circulation. During the interglacial period, owing to cold bottom currents, sediments containing abundant chlorite were transported to the Ulleung Basin (Ohta et al., 2013; Hyun et al., 2022). Therefore, kaolinite and chlorite in the basin are associated with several factors, including the climate, ocean circulation, and sediment source.

4.3. Elemental Composition of Smectite

Smectite samples that are representative of each area of provenance were analyzed, and the SAED and EDS data are displayed in Figure 7. Owing to its hair-like morphology, smectite was distinct from other clay minerals EDS analysis revealed a lattice fringe in the smectite with an SAED mean d_{100} of 1.35 nm and a mean

https://doi.org/10.1007/s12303-023-0011-z

Table 2. Relative abundances of clay minerals in the piston-core sediments from St. 8

Sample site	Depth (cm)	Smectite (%)		Illite (%)		Kaolinite (%)		Chlorite (%)	
		avg	std	avg	std	avg	std	avg	std
St. 8	5	27.3	0.13	63.4	0.32	4.2	0.03	5.2	0.04
	35	42.1	0.37	49.1	0.27	3.4	0.04	5.4	0.07
	65	38.8	0.09	50.1	0.18	5.2	0.12	5.9	0.14
	95	45.2	0.10	47.5	0.19	3.4	0.05	3.9	0.06
	125	42.1	0.41	49.4	0.32	3.1	0.07	5.4	0.12
	155	48.8	0.19	37.7	0.28	8.0	0.15	5.6	0.10
	160	49.6	0.31	39.4	0.17	4.4	0.06	6.6	0.09
	176	21.2	0.49	53.1	0.47	12.7	0.08	13.0	0.08
	185	20.2	0.47	59.6	0.56	10.4	0.20	9.8	0.19
	215	31.2	0.25	55.3	0.49	6.9	0.13	6.6	0.12
	223	37.2	0.13	51.5	0.23	6.6	0.15	4.7	0.10
	245	16.9	0.05	63.8	0.34	7.1	0.11	12.3	0.18
	253	33.8	0.24	47.4	0.51	7.4	0.11	11.4	0.18
	275	29.5	0.40	59.4	0.31	5.1	0.11	6.0	0.13
	305	27.6	0.12	56.8	0.49	8.1	0.30	7.5	0.28
	335	39.4	0.05	48.8	0.27	5.8	0.12	6.0	0.13
	365	28.9	0.49	55.4	0.08	8.5	0.23	7.2	0.19
	395	34.6	0.21	49.9	0.06	7.6	0.08	7.8	0.08
	399	47.6	0.52	36.0	0.20	10.0	0.44	6.4	0.28
	425	29.4	0.39	51.0	0.57	9.8	0.09	9.8	0.09
	443	13.8	0.35	56.5	1.21	16.1	0.48	13.5	0.40
	455	13.4	0.30	64.2	0.23	9.1	0.05	13.3	0.07
	485	18.8	0.32	60.8	0.33	11.6	0.11	8.7	0.08
	503	14.4	0.04	57.7	0.55	16.1	0.30	11.8	0.22
	515	10.1	0.71	63.4	2.48	18.8	1.26	7.7	0.51
	545	12.5	0.23	59.7	0.11	12.1	0.08	15.7	0.10

Note: avg, average; std, standard deviation.

Al/Si ratio of 0.36 (Kim et al., 2004).

Elemental compositions of smectites that were analyzed are displayed using an Al-Mg-Fe ternary diagram in Figure 8. Evidently, Al exhibits the highest relative proportion, and its concentration varies from 0.3 to 0.9 wt%, excluding for five samples. In addition, Al displays a strong negative correlation with Fe, and concentrations of Mg are generally less than 0.15 wt%.

Smectites in samples from different stations involve montmorillonite-beidellite (Al-rich, Area 1), trioctahedral (saponite, Mg-rich, Area 2), and nontronite (Fe-rich, Area 3) types, and data for the samples analyzed are composed with data for smectites in samples from the Dokdo using a ternary diagram (Fig. 8; Weaver and Pollard, 2011; Lee et al., 2020). Smectite is widely distributed in Areas 1 and 3, with montmorillonite and nontronite being dominant, whereas saponite is rare in the surface sediments from the Ulleung Basin. Smectites for the samples analyzed can be divided into Fe-rich and Al-rich smectites. Compared to samples from the Dokdo (Al = 32.9%, Fe = 33.3%, and Mg = 33.8%; Lee et al., 2020), the samples analyzed in the present study are richer in Al and Fe (Al = 50.4%, Fe = 40.2%, and Mg = 9.4%), and thus, these exhibit no significant correlation.

Evidently, data for samples attributed to a common origin are comparable and differ from those of other sources. Samples from stations associated with the Korean coast and TWC show that Fe and Mg abundances increase from St. 2 to St. 5 and from St. 9 to St. 10, respectively. Conversely, data for samples from stations that were assigned a mixed provenance in display no trend, except for the highest Al concentration for the sample from St. 8. However, differences in the elemental composition of smectites according to the area of origin were not evident. Hence, in addition to the three sources, smectites were probably contributed to the basin from other sources or mechanism.

The interlayer cation (K-Ca-Na) composition of samples that were plotted in a ternary diagram (Fig. 9) revealed high relative proportions of K (0.4–0.8 wt%), whereas the proportion of Na varied from 0.1 to 0.4 wt% and that of Ca was mostly less than 0.4 wt%. Data for samples that originated from the Korean coast show no distinct pattern because Na data for samples from St. 3,

Table 3. Relative abundances of clay minerals in the piston-core sediments from St. 10

Sample site	Depth (cm)	Smectite (%)		Illite (%)		Kaolinite (%)		Chlorite (%)	
		avg	std	avg	std	avg	std	avg	std
St. 10	5	27.4	0.02	62.4	0.06	4.4	0.02	5.8	0.03
	35	41.7	0.11	50.2	0.32	3.5	0.10	4.5	0.12
	65	36.9	0.24	53.0	0.11	4.5	0.07	5.6	0.09
	95	31.0	0.27	55.1	0.47	6.4	0.13	7.5	0.15
	125	34.4	0.62	53.1	0.52	5.4	0.06	7.2	0.09
	155	33.7	0.25	59.8	0.57	3.4	0.18	3.1	0.16
	185	40.3	0.22	44.4	0.10	7.9	0.12	7.4	0.11
	215	30.8	0.27	55.2	0.29	7.2	0.05	6.7	0.05
	245	27.2	0.25	57.4	0.46	7.2	0.15	8.2	0.17
	275	31.0	0.13	58.5	0.06	4.1	0.02	6.3	0.04
	280	36.8	0.38	48.7	0.35	7.9	0.04	6.6	0.04
	305	27.4	0.07	53.7	0.28	9.8	0.11	9.1	0.10
	335	31.5	0.45	54.9	0.67	7.5	0.17	6.1	0.14
	353.5	28.8	0.26	62.3	0.38	4.1	0.29	4.9	0.34
	365	32.6	0.17	53.2	0.26	7.0	0.07	7.2	0.07
	395	30.1	0.33	51.2	0.44	7.5	0.08	11.2	0.13
	403	27.0	0.04	60.5	0.07	6.3	0.05	6.3	0.05
	425	29.1	0.15	60.3	0.15	5.2	0.00	5.3	0.00
	455	36.2	0.21	55.4	0.40	3.9	0.12	4.4	0.14
	485	28.7	0.21	52.5	0.22	9.1	0.19	9.6	0.20
	490	29.6	0.06	53.8	0.41	8.9	0.21	7.7	0.18
	515	29.6	0.12	55.3	0.15	8.3	0.02	6.8	0.01
	541	26.1	0.33	56.8	0.13	8.8	0.10	8.4	0.10
	545	18.2	0.33	53.5	0.69	14.0	0.18	14.4	0.19
	575	28.0	0.27	52.6	0.21	8.3	0.20	11.2	0.27
	605	25.5	0.16	56.0	0.25	7.8	0.11	10.7	0.15
	619	19.0	0.20	62.3	0.21	9.0	0.12	9.6	0.12
	628	19.1	0.09	59.5	0.16	11.1	0.10	10.2	0.09
	630	22.7	0.09	57.1	0.19	8.3	0.05	11.9	0.07

Note: avg, average; std, standard deviation.

for example, cover the entire range for all samples. In contrast, data for samples that are assigned to the TWC reveal that the concentration of K increases from St. 9 to St. 10, whereas the concentrations of Ca for samples from St. 10 are very low. Regarding the samples of a mixed provenance, the concentration of K increases from St. 5 and St. 6, whereas samples from St. 7 show K concentrations that are lower than those from St. 5. Therefore, even though the proportions of K in Figure 9 are relatively high, the concentrations of K for the samples are lower while the concentrations of Fe are higher than those associated with glauconitization (Fig. S2 in the electronic supplementary material; López-Quirós et al., 2019). Consequently, most of the samples analyzed are considered K-poor smectites (Fig. S3 in the electronic supplementary material; Ransom and Helgeson, 1993). The relatively low K concentrations of the samples can be attributed to a selective incorporation in the sediments, which in addition to smectite, were characterized by high-net-negative-charges because of other clay minerals (Hover et al., 2002).

5. CONCLUSIONS

In the present study, the mineralogy, geochemistry and sources of clay minerals in sediments of the Ulleung Basin, East Sea, were investigated. The results revealed that smectite originated primarily from the Korean coast, whereas illite was mainly sourced from the TWC. The main sediment source changed from terrigenous to hemipelagic in the Holocene, with similar trends in the proportions of kaolinite and chlorite in the sediments. The composition of clay minerals in the sediments studied was affected by several factors of the climate, ocean circulation, and sediment source. TEM-EDS observations showed that the smectites can be divided into two groups (Al-rich and Fe-rich), and these

https://doi.org/10.1007/s12303-023-0011-z

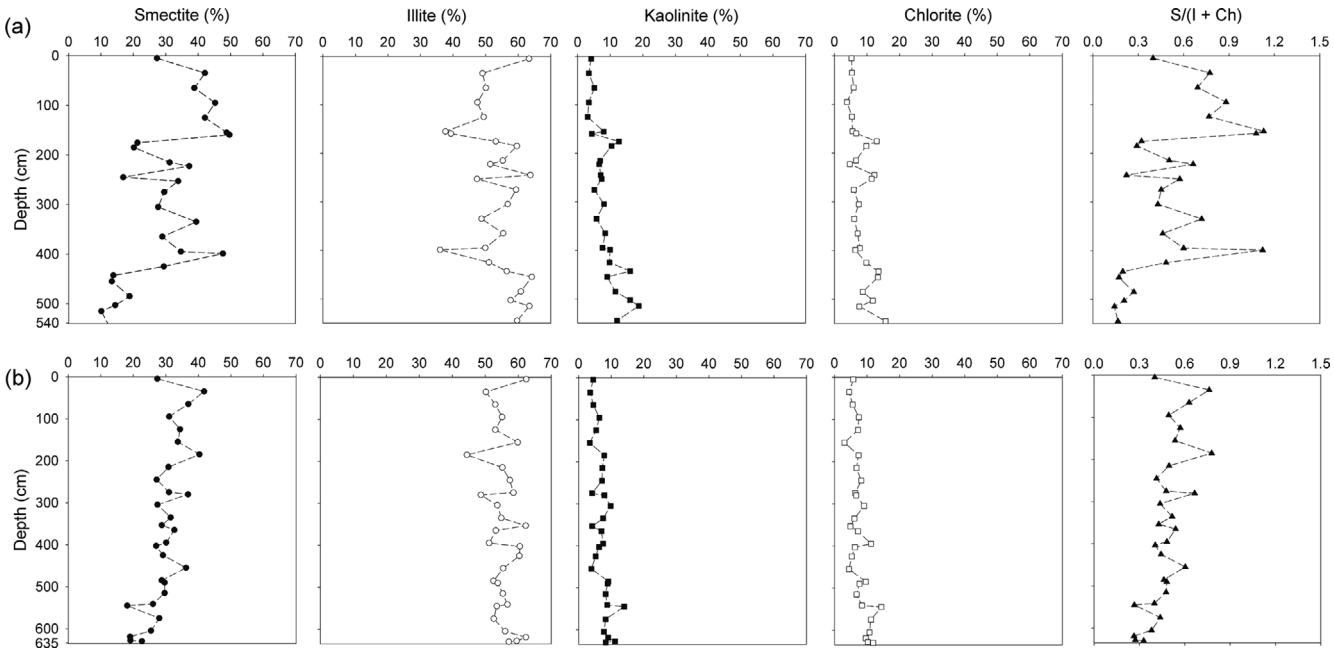

Fig. 6. Vertical trends of the relative abundances of clay minerals at (a) St. 8 and (b) St. 10. S – Smectite, I – Illite, and Ch – Chlorite.

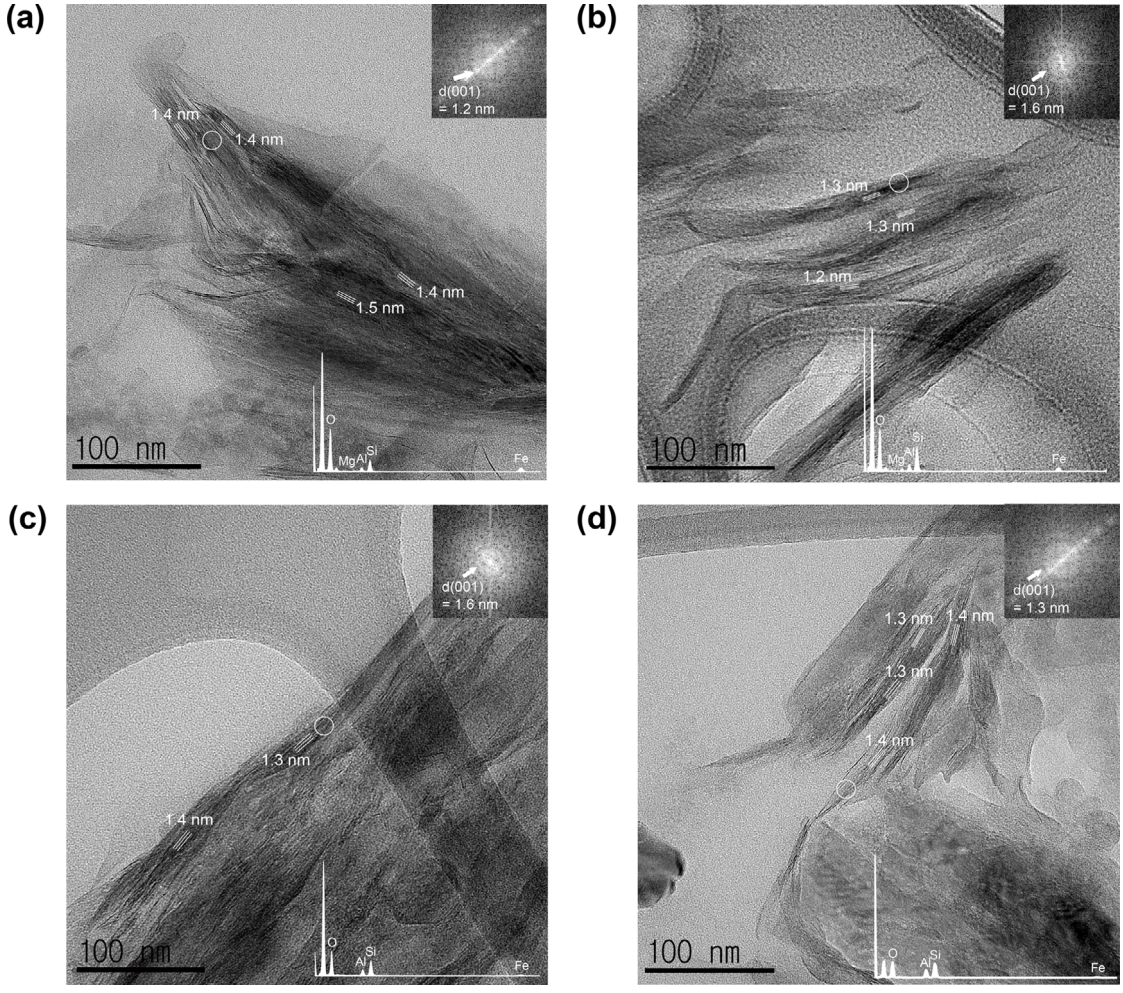

Fig. 7. Representative transmission electron microscopy (TEM) images of smectites of three origins based on selected-area electron diffraction and energy dispersive X-ray spectroscopy (EDS) including (a) St. 1, assigned to a mixed provenance, (b) St. 2, from the Korean coast, (c) St. 7, assigned to a mixed source, and (d) St. 10, linked to the TWC. The elemental compositions of the smectites were determined using TEM-EDS.

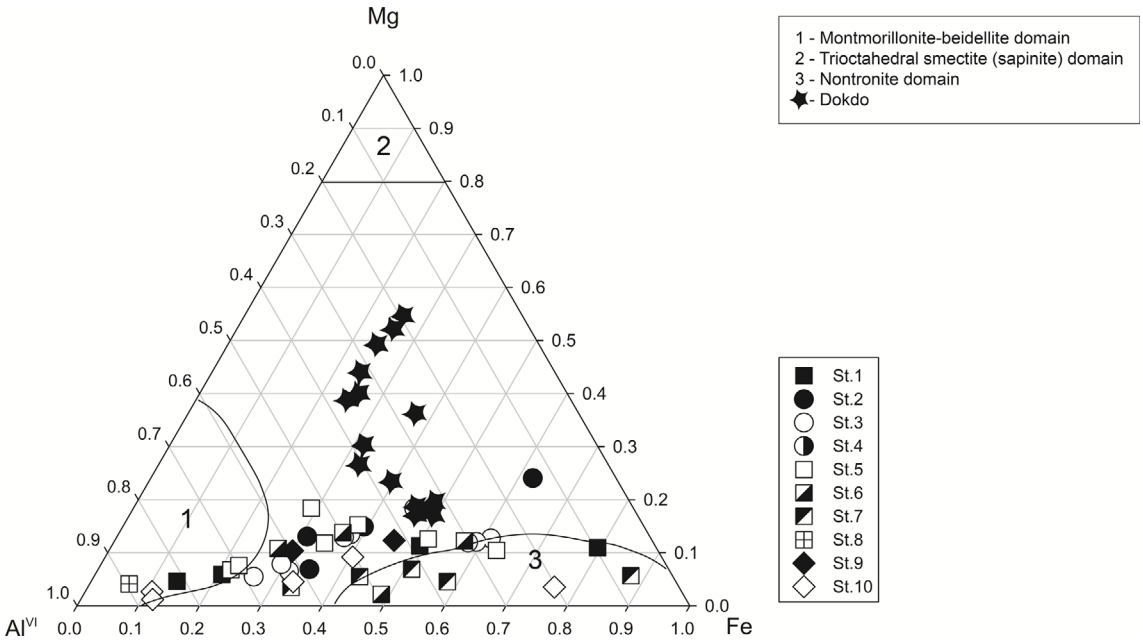

Fig. 8. Ternary diagram (Al-Fe-Mg) associated with elements at octahedral sites in smectites from surface sediments in the Ulleung Basin (modified from Lee et al., 2020). The circle (●) indicates a source from the Korean coast, the diamond (◆) indicates an origin from the TWC, and a square (■) highlights a mixed provenance. Area 1 is associated with montmorillonite-beidellite, Area 2 is linked to trioctahedral smectite (saponite), and Area 3 involves nontronite (Weaver and Pollard, 1973). The star (★) indicates a sample from Dokdo (Lee et al., 2020). Evidently, smectite is widely distributed in Areas 1 and 3.

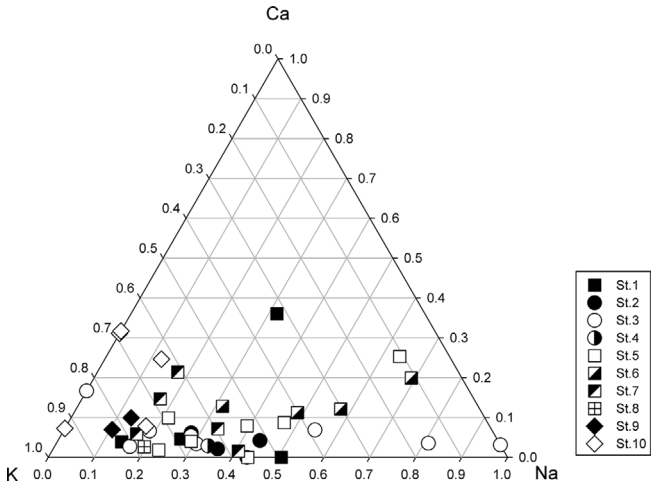

Fig. 9. Ternary diagram (K-Ca-Na) associated with cation sites in smectites from surface sediments in the Ulleung Basin. The circle (●) indicates a provenance from the Korean coast, the diamond (◆) denotes a source from the TWC, and the Square (■) represents a mixed provenance.

were reflective of changes in the provenance of the associated sediments. In addition to three sources highlighted in the present study, multiple other sources likely contributed to the composition of the sediments that were studied. In contrast to previous studies, in the present study, TEM-EDS enabled classification of the sediments according to sources. Most of the Korean coast smectite was located in montmorillonite-beidellite and nontronite areas, whereas that of the TWC was located between these two areas. Findings of the present study indicate that factors such as climate, ocean currents, and sediment sources interact with each other and affect clay mineral distribution. This is not consistent with previous studies that eolian dusts are the primary source of sediments. In addition, our findings improve the understanding of the composition and origin of sediments in the Ulleung Basin, East Sea.

ACKNOWLEDGMENTS

This work was supported by a 2-Year Research Grant of Pusan National University.

REFERENCES

Bahk, J.J., Chough, S.K., Jeong, K.S., and Han, S.J., 2001, Sedimentary records of paleoenvironmental changes during the last deglaciation in the Ulleung Interplain Gap, East Sea (Sea of Japan). Global and Planetary Change, 28, 241–253.

Bahk, J.J., Han, S.J., and Khim, B.K., 2004, Variations of terrigenous sediment supply to the southern slope of the Ulleung Basin, East/Japan Sea since the Last Glacial Maximum. Geosciences Journal, 8, 381–390.

Bahk, J.J., Lee, S.H., Yoo, H.S., Back, G.G., and Chough, S.K., 2005, Late Quaternary sedimentary processes and variations in bottom-current activity in the Ulleung Interplain Gap, East Sea (Korea).

https://doi.org/10.1007/s12303-023-0011-z

Marine Geology, 217, 119–142.
Biscaye, P.E., 1965, Mineralogy and sedimentation of recent deep-sea clay in the Atlantic Ocean and adjacent seas and oceans. Geological Society of America Bulletin, 76, 803–832.
Cha, H.J., Choi, M.S., Lee, C.B., and Shin, D.H., 2007, Geochemistry of surface sediments in the southwestern East/Japan Sea. Journal of Asian Earth Sciences, 29, 685–697.
Hover, V.C., Walter, L.M., and Peacor, D.R., 2002, K uptake by modern estuarine sediments during early marine diagenesis, Mississippi Delta Plain, Louisiana, USA. Journal of Sedimentary Research, 72, 775–792.
Hyun, S.M., Kim, J.K., Kang, J.W., and Kim, G.Y., 2022, Multi-proxy stratigraphy and paleoceanographic variations in sediment from the Korea Plateau, East Sea (Japan Sea), Over the Last 500 kyr. Ocean Science Journal, 57, 420–435.
Irino, T. and Tada, R., 2003, High-resolution reconstruction of variation in aeolian dust (Kosa) deposition at ODP site 797, the Japan Sea, during the last 200 ka. Global and Planetary Change, 35, 143–156.
Khim, B.K., Shin, D.H., and Han, S.J., 1997, Organic carbon, calcium carbonate, and clay mineral distributions in the Korea Strait region, the southern part of the East Sea. Journal of the Korean Society of Oceanography, 32, 128–137.
Kim, G.Y. and Kim, D.C., 2001, Comparison and correlation of physical properties from the plain and slope sediments in the Ulleung Basin, East Sea (Sea of Japan). Journal of Asian Earth Sciences, 19, 669–681.
Kim, J.W., Dong, H., Seabaugh, J., Newell, S.W., and Eberl, D.D., 2004, Role of microbes in the smectite-to-illite reaction. Science, 303, 830–832.
Kim, J.W., Dong, H., Yang, K.H., Park, H.B., Elliott, W.C., Spivack, A., Koo, T.H., Kim, G.Y., Morono, Y., and Henkel, S., 2019, Naturally occurring, microbially induced smectite-to-illite reaction. Geology, 47, 535–539.
Kim, J.W., Peacor, D.R., Tessier, D., and Elsass, F., 1995, A technique for maintaining texture and permanent expansion of smectite interlayers for TEM observations. Clays and Clay Minerals, 43, 51–57.
Koo, B.Y., Kim, S.P., Lee, G.S., and Chung, G.S., 2014, Seafloor morphology and surface sediment distribution of the southwestern part of the Ulleung Basin, East Sea. Journal of the Korean Earth Science Society, 35, 131–146. (in Korean with English abstract) https://doi.org/10.5467/JKESS.2014.35.2.131
Kwak, K.Y., Choi, H.S., and Cho, H.G., 2016, Paleo-environmental change during the late Holocene in the southeastern Yellow Sea, Korea. Applied Clay Science, 134, 55–61. https://doi.org/10.1016/j.clay.2016.05.007
Lee, B.K. and Kim, S.Y., 2007, Sedimentary facies and processes in the Ulleung Basin and southern East Sea. Korean Journal of Fisheries and Aquatic Sciences, 40, 160–166. (in Korean with English abstract) https://doi.org/10.5657/kfas.2007.40.3.160
Lee, K.E., 2007, Surface water changes recorded in Late Quaternary marine sediments of the Ulleung Basin, East Sea (Japan Sea). Palaeogeography, Palaeoclimatology, Palaeoecology, 247, 18–31.
Lee, K.H., Kim, C.H., Park, C.H., Yang, K., Lee, S.H., Lee, I.S., Kwack, Y.J., Kwak, J.W., Jung, J.W., and Kim, J.W., 2020, Microbial diversity responding to changes in depositional conditions during the last glacial and interglacial period: NE Ulleung Basin, East Sea (Sea of Japan). Minerals, 10, 208.
Lee, S.H., Jou, H.T., Bahk, J.J., Jun, H.G., Moon, S.H., Kim, H.J., Horozal, S., Cukur, D., Um, I.K., and Yoo, D.G., 2021, Latest Quaternary mass-transport processes of fan-shaped body in the western margin of the Ulleung Basin, East Sea (Japan Sea). Geosciences Journal, 25, 93–105.
Lee, S.J., Kim, C.H., Jun, C.P., Lee, S.J., and Kim, Y.K., 2015, Mineralogical characteristics of marine sediments cores from Uleung Basin and Hupo Basin, East Sea. Journal of the Mineralogical Society of Korea, 28, 71–81. (in Korean with English abstract)
Lim, D.I., Xu, Z., Choi, J.Y., Kim, S.Y., Kim, E.H., Kang, S.R., and Jung, H.S., 2011, Paleoceanographic changes in the Ulleung Basin, East (Japan) Sea, during the last 20,000 years: evidence from variations in element composition of core sediments. Progress in Oceanography, 88, 101–115.
Liu, Y., Sha, L., Shi, X., Suk, B.C., Li, C., Wang, K., and Li, X., 2010, Depositional environment in the southern Ulleung Basin, East Sea (Sea of Japan), during the last 48 000 years. Acta Oceanologica Sinica, 29, 52–64.
López-Quirós, A., Escutia, C., Sánchez-Navas, A., Nieto, F., Garcia-Casco, A., Martín-Algarra, A., Evangelinos, D., and Salabarnada, A., 2019, Glaucony authigenesis, maturity and alteration in the Weddell Sea: an indicator of paleoenvironmental conditions before the onset of Antarctic glaciation. Scientific Reports, 9, 1–12.
Mooers, C.N., Bang, I., and Sandoval, F.J., 2005, Comparisons between observations and numerical simulations of Japan (East) Sea flow and mass fields in 1999 through 2001. Deep Sea Research Part II: Topical Studies in Oceanography, 52, 1639–1661.
Moore, D.M. and Reynolds Jr., R.C., 1989, X-ray Diffraction and the Identification and Analysis of Clay Minerals. Oxford University Press, Oxford, United Kingdom, 332 p.
Nagashima, K., Tada, R., Tani, A., Sun, Y., Isozaki, Y., Toyoda, S., and Hasegawa, H., 2011, Millennial-scale oscillations of the westerly jet path during the last glacial period. Journal of Asian Earth Sciences, 40, 1214–1220.
Ohta, A., Imai, N., Terashima, S., Tachibana, Y., and Ikehara, K., 2013, Regional spatial distribution of multiple elements in the surface sediments of the eastern Tsushima Strait (southwestern Sea of Japan). Applied Geochemistry, 37, 43–56. https://doi.org/10.1016/j.apgeochem.2013.06.010
Park, K.A., Park, J.E., Choi, B.J., Byun, D.S., and Lee, E.I., 2013, An oceanic current map of the East Sea for science textbooks based on scientific knowledge acquired from oceanic measurements. The Sea: Journal of The Korean Society of Oceanography, 18, 234–265. (in Korean with English abstract) https://doi.org/10.7850/jkso.2013.18.4.234
Ransom, B. and Helgeson, H.C., 1993, Compositional end members and thermodynamic components of illite and dioctahedral aluminous smectite solid solutions. Clays and Clay minerals, 41, 537–550.
Sagawa, T., Nagahashi, Y., Satoguchi, Y., Holbourn, A., Itaki, T., Gallagher, S.J., Saavedra-Pellitero, M., Ikehara, K., Irino, T., and Tada, R., 2018, Integrated tephrostratigraphy and stable isotope stratigraphy in the Japan Sea and East China Sea using IODP Sites U1426, U1427, and U1429, Expedition 346 Asian Monsoon. Progress in Earth and

Planetary Science, 5, 1–24. https://doi.org/10.1186/s40645-018-0168-7

Shen, X., Wan, S., France-Lanord, C., Clift, P.D., Tada, R., Révillon, S., Shi, X., Zhao, D., Liu, Y., and Yin, X., 2017, History of Asian eolian input to the Sea of Japan since 15 Ma: links to Tibetan uplift or global cooling? Earth and Planetary Science Letters, 474, 296–308.

Son, B.K., Kim, H.J., and Ahn, G.O., 2009, Mineral composition of the sediment of Ulleung Basin, Korea. Journal of the Mineralogical Society of Korea, 22, 115–127. (in Korean with English abstract)

Um, I.K., Choi, M.S., Bahk, J.J., and Song, Y.H., 2013, Discrimination of sediment provenance using rare earth elements in the Ulleung Basin, East/Japan Sea. Marine Geology, 346, 208–219.

Weaver, C.E. and Pollard, L.D., 1973, The Chemistry of Clay Minerals (1st edition). Elsevier, Amsterdam, Netherlands, 224 p.

Xu, Z., Lim, D.I., Choi, J.Y., Li, T., Wan, S., and Rho, K.C., 2014, Sediment provenance and paleoenvironmental change in the Ulleung Basin of the East (Japan) Sea during the last 21 kyr. Journal of Asian Earth Sciences, 93, 146–157.

Yokoyama, Y., Naruse, T., Ogawa, N.O., Tada, R., Kitazato, H., and Ohkouchi, N., 2006, Dust influx reconstruction during the last 26,000 years inferred from a sedimentary leaf wax record from the Japan Sea. Global and Planetary Change, 54, 239–250.

https://doi.org/10.1007/s12303-023-0011-z